

DNA Repair Factor APLF Is a Histone Chaperone

Pawan Vinod Mehrotra,¹ Dragana Ahel,¹ Daniel P. Ryan,² Ria Weston,¹ Nicola Wiechens,² Rolf Kraehenbuehl,¹ Tom Owen-Hughes,² and Ivan Ahel^{1,*}

¹Cancer Research UK, Paterson Institute for Cancer Research, University of Manchester, Wilmslow Road, Manchester M20 4BX, UK

²Wellcome Trust Centre for Gene Regulation and Expression, College of Life Sciences, University of Dundee, Dundee DD1 5EH, UK

*Correspondence: iaheh@picr.man.ac.uk

DOI 10.1016/j.molcel.2010.12.008

SUMMARY

Poly(ADP-ribosylation) plays a major role in DNA repair, where it regulates chromatin relaxation as one of the critical events in the repair process. However, the molecular mechanism by which poly(ADP-ribose) modulates chromatin remains poorly understood. Here we identify the poly(ADP-ribose)-regulated protein APLF as a DNA-damage-specific histone chaperone. APLF preferentially binds to the histone H3/H4 tetramer via its C-terminal acidic motif, which is homologous to the motif conserved in the histone chaperones of the NAP1L family (NAP1L motif). We further demonstrate that APLF exhibits histone chaperone activities in a manner that is dependent on its acidic domain and that the NAP1L motif is critical for the repair capacity of APLF *in vivo*. Finally, we identify structural analogs of APLF in lower eukaryotes with the ability to bind histones and localize to the sites of DNA-damage-induced poly(ADP-ribosylation). Collectively, these findings define the involvement of histone chaperones in poly(ADP-ribose)-regulated DNA repair reactions.

INTRODUCTION

The repair of DNA strand breaks is critical for genome integrity; therefore living cells have evolved a variety of response mechanisms to efficiently repair damaged DNA. One of the critical protein modifications that regulates DNA break repair in higher eukaryotes is poly(ADP-ribosylation). Poly(ADP-ribose) (PAR) is a highly negatively charged polymer consisting of repeating ADP-ribose units and is synthesized by the PARP family of enzymes using NAD⁺ as a substrate (D'Amours *et al.*, 1999). The principal PARP involved in DNA damage recognition and signaling is poly(ADP-ribose) polymerase 1 (PARP1). PARP1 is activated by DNA strand breaks and catalyzes the poly(ADP-ribosylation) of target proteins, including PARP1 itself and histones, around DNA breaks (Kim *et al.*, 2005). This local increase in poly(ADP-ribosylation) serves as a specific signal for the recruitment of a number of repair proteins that recognize PAR using specific PAR-interaction modules (Pleschke *et al.*,

2000; Karras *et al.*, 2005; Ahel *et al.*, 2008). In addition, as a consequence of poly(ADP-ribosylation) by PARP1, chromatin adopts a more relaxed structure, thereby increasing lesion accessibility and repair efficiency (Poirier *et al.*, 1982). One of the recently identified factors involved in this process is a chromatin remodeler ALC1 (Ahel *et al.*, 2009). However, the molecular mechanisms by which PAR modulates chromatin structure in response to DNA damage are still largely unresolved.

Recently, Aprataxin-PNK-like factor (APLF, also referred to as Xip1 and PALF) has been identified as a damage response factor with a particularly high binding affinity for poly(ADP-ribose) (Iles *et al.*, 2007; Kanno *et al.*, 2007; Ahel *et al.*, 2008). Downregulation of APLF in human cells leads to an apparent cellular sensitivity to various DNA damaging agents (Iles *et al.*, 2007; Bekker-Jensen *et al.*, 2007). APLF is recruited to the sites of DNA damage by binding to poly(ADP-ribosylated) PARP1 protein via a tandem of poly(ADP-ribose)-binding zinc-finger (PBZ) motifs (Ahel *et al.*, 2008; Eustermann *et al.*, 2010) (Figure 1A). The inhibition of PAR synthesis using specific PARP inhibitors abolishes this recruitment (Bekker-Jensen *et al.*, 2007). Furthermore, APLF is constitutively associated with DNA repair ligase complexes through a direct interaction with the main scaffolding proteins XRCC1 and XRCC4 (Iles *et al.*, 2007; Macrae *et al.*, 2008). These interactions are mediated by APLF's N-terminal FHA domain. Finally, APLF possesses a conserved domain of unknown function at its C terminus, which is rich in acidic residues (Figure 1A). Complementation experiments have shown that the acidic C-terminal domain is vital for APLF's activity in DNA repair (Rulten *et al.*, 2008), suggesting that understanding the function of this domain may be the key to elucidating the exact role of APLF in DNA repair.

RESULTS AND DISCUSSION

APLF Shares Homology with the NAP1-like Family of Histone Chaperones

To gain a further insight into the function of the acidic C-terminal domain, we performed homology searches through available databases using the primary sequence of the last 70 residues of human APLF, to identify whether homologous modules exist in other proteins. Interestingly, the search revealed that the whole acidic domain of APLF is integrated into the XRCC1 protein of slime molds (Figure 4A), which notably lack an APLF ortholog. In addition, we found a short acidic motif with two conserved prolines and several large hydrophobic residues

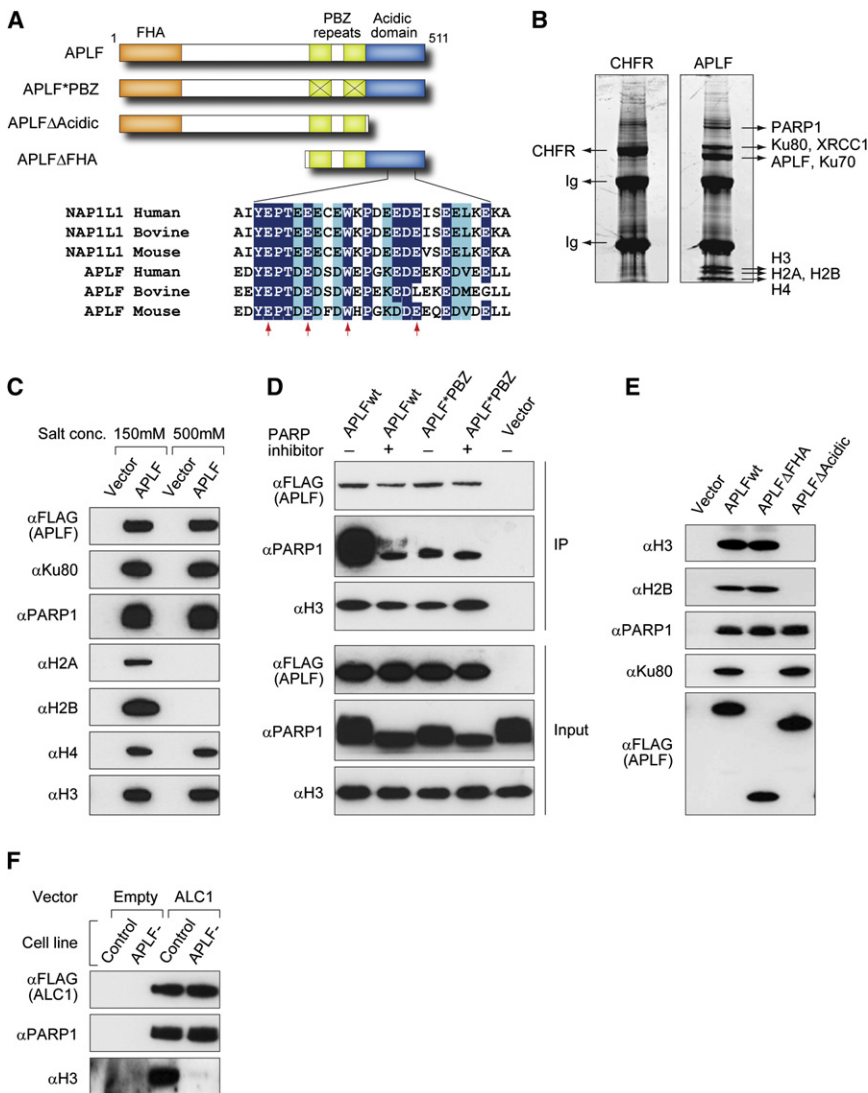


Figure 1. APLF Interacts with Core Histones

(A) Complexes were purified by immunoprecipitation of transiently expressed FLAG-tagged proteins in HEK293T cells. In (A), schematic representation of the APLF domain structure and detailed alignment of the conserved motif within the acidic C-terminal domain homologous to the NAP1-like family of histone chaperones (NAP1L motif) is shown. Various mutant constructs used in the studies are shown separately. Point mutants in the NAP1L motif are indicated by red arrows. (B) SyproRuby staining of the immunoprecipitated APLF complex. Relevant interactors identified by mass spectrometry are shown separately. (C) Immunoblot confirming the interaction of APLF with core histones at low and high salt stringency. (D) The interaction of APLF with core histones is independent of poly(ADP-ribosylation). (E) Interaction of APLF with core histones is mediated by the acidic C-terminal domain. (F) The presence of histones in ALC1-associated complexes is dependent on APLF.

within the C-terminal domain of APLF that share a striking similarity with a motif present in the nucleosome assembly protein 1 (NAP1)-like protein family of histone chaperones (Figure 1A). We have named this motif the “NAP1L motif,” for NAP1-like motif. In NAP1-like proteins, the NAP1L motif is positioned within their central domain, which is critical for chaperone activity; however, the exact function of the NAP1L motif is currently unclear (Park and Luger, 2006a). One of the best-characterized members of NAP1-like family is the *Drosophila* NAP1 protein, which is suggested to serve as a chaperone for various chromatin remodellers in ATP-dependent chromatin assembly (Lusser et al., 2005).

APLF Binds Core Histones via Its Acidic Domain

The acidic nature of APLF’s C terminus and the similarity of its NAP1L motif to histone chaperones suggests that the C terminus may mediate interactions with histones. Therefore, our first approach was to analyze APLF-associated proteins

in HEK293T cells. To achieve this, we transiently expressed FLAG-tagged APLF and purified complexes from cell extracts using FLAG-agarose beads. In order to exclude nonspecific PAR-mediated interactions, we used FLAG-tagged CHFR (another protein that is known to bind strongly to PAR) as a control pull-down (Ahel et al., 2008). Comparative mass-spectrometry analysis confirmed previously known APLF interactions, for example with the Ku heterodimer, PARP1, and XRCC1. Interestingly, we also detected the presence of all four core histones in the APLF immunoprecipitates (Figure 1B), and these interactions were confirmed by western blotting using specific anti-histone antibodies (Figure 1C). We assessed the stability of the APLF-histone interaction by performing immunoprecipitation in more stringent salt conditions. This experiment revealed that APLF interacts strongly with H3/H4 and showed that the interaction is stable up to 0.5 M NaCl. Conversely, interactions with H2A and H2B were less salt tolerant (Figure 1C). Next, we observed that the interaction of APLF with histones is not poly(ADP-ribose)-dependent, as the treatment of HEK293T cells with a specific PARP inhibitor did not affect the histone-binding capacity of APLF (Figure 1D). Similarly, mutation of APLF’s PBZ domains does not affect the presence of histones in our pull-downs (Figure 1D). In contrast, immunoprecipitations using truncated APLF variants revealed that the acidic C-terminal domain is necessary for the interaction with core histones (Figure 1E). Collectively, these results demonstrate that APLF exhibits a stable interaction with core histones, which is independent of poly(ADP-ribosylation) and is mediated by the acidic C terminus of APLF. Interestingly, although DNA repair

proteins have to operate within histone contexts, histone-binding motifs have not been characterized to date, in the core factors involved in mammalian DNA break repair.

APLF Is a Major Histone-binding Component in the ALC1-associated Complex

We have recently shown that APLF also interacts with the DNA repair protein ALC1 in vivo, along with several other DNA repair factors such as PARP1, Ku-heterodimer, XRCC1, and core histone components (Ahel et al., 2009). ALC1 is a chromatin remodeler of the SWI/SNF2 family (Flaus et al., 2006) and is the only chromatin remodeler shown so far to be directly involved in mammalian DNA repair. We therefore wanted to assess whether the ability of the ALC1-associated complex to bind histones is dependent on the presence of APLF. To do this, we stably down-regulated APLF expression using shRNA technology in human U2OS cells and analyzed the ALC1-associated complexes by immunoprecipitating transiently expressed FLAG-tagged ALC1 from the U2OS cell extracts. Interestingly, the results showed that the ability of ALC1 to interact with histones is dependent on the presence of APLF (Figure 1F). In contrast, the ability of ALC1 to bind PARP1 was not affected in APLF-depleted cells. Thus, APLF represents the major storage storage protein for soluble histones in the DNA repair complex. APLF's role in the association of histones with ALC1 raises the possibility that there is a functional interaction between these proteins. We were therefore able to demonstrate that APLF negatively regulates PARP1-dependent ATPase activation of ALC1 in vitro, but this effect is independent of the acidic domain, and instead is dependent on the PBZ repeat region of APLF (Figure S1).

The NAP1L Motif of APLF Is Critical for Interaction with the H3/H4 Tetramer

To confirm direct interactions between APLF and core histones, we carried out an in vitro GST-pull-down experiment. We purified GST-tagged versions of APLF from *E. coli* (Figure 2A) and performed pull-downs using reconstituted H3/H4 tetramers or H2A/H2B dimers in the presence of 0.6 M salt. Under these conditions APLF did not bind to H2A/H2B, but exhibited binding to H3/H4. Thus, APLF binds to the tetramer directly. Importantly, the APLF-tetramer interaction was completely abolished by deleting the acidic C terminus of APLF, consistent with the in vivo interaction results (Figure 2B). In addition, the interaction was also abrogated by mutating a single conserved tryptophan (W485) residue within the NAP1L motif (Figure 2B). For this reason, we analyzed which of the specific residues in the APLF NAP1L motif are critical for binding to the H3/H4 tetramer. To do this, we performed an alanine-scanning mutagenesis of several conserved residues within the motif (Figure 1A) and assessed the ability of these mutants to bind histones in vivo using FLAG-tag pull-downs. The result revealed that mutations of E477 and W485 greatly affected the binding of APLF to H3/H4 at 0.5 M salt (Figure 2C). Encouraged by this result, we proceeded to examine whether analogously to APLF, the binding of H3/H4 by human NAP1L1 protein is also dependent on the NAP1L motif. NAP1L1-histone interactions in vivo are less stable than for APLF-histone interactions, and the immunoprecipita-

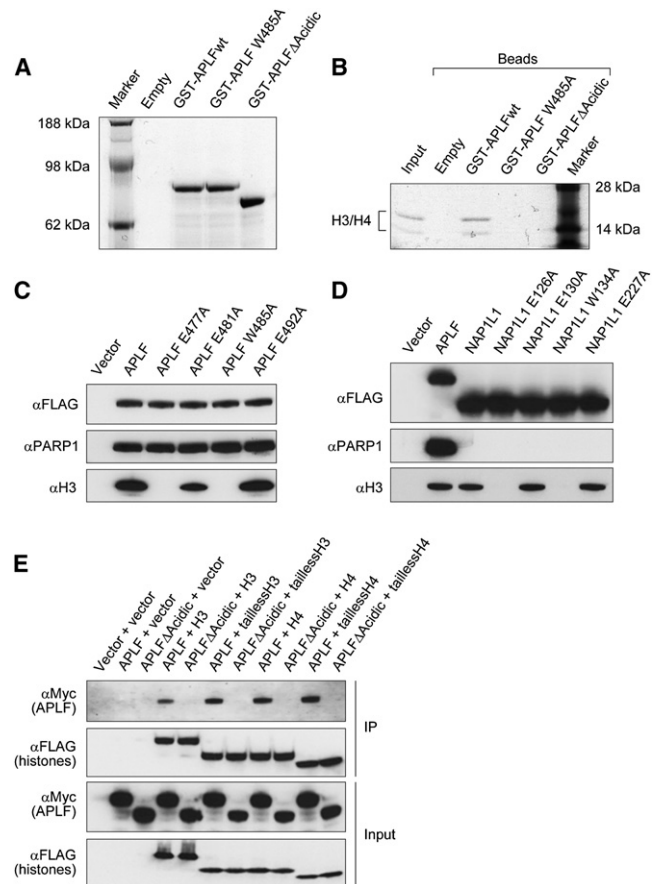


Figure 2. Mode of H3/H4 Recognition by APLF Resembles NAP1 Family of Histone Chaperones

(A) Coomassie-stained gel showing purified GST-tagged APLF proteins. (B) Binding of purified H3/H4 tetramer by GST-tagged APLF variants in vitro. (C) Mutation of specific residues within the NAP1L-motif of APLF reduces its interaction with H3/H4 in vivo. (D) Mutation of specific residues within the NAP1L-motif of human NAP1L1 abolishes its interaction with H3/H4 in vivo. (E) APLF binds to the globular region of H3 and H4 through its acidic C terminus. In Figures 2C, 2D, and 2E, the in vivo complexes were purified by immunoprecipitation of transiently expressed FLAG-tagged proteins in HEK293T cells and analyzed by western blotting.

tion experiments were in this case performed at 150 mM NaCl. When we compared the immunoprecipitates of transiently expressed human NAP1L1 WT and corresponding NAP1L1 mutants for the presence of histone H3, we observed the same pattern as seen for APLF (Figure 2D). Again, the binding was abrogated by the mutation of a single glutamate or tryptophan residue (residues 126 and 134, respectively), demonstrating that APLF and NAP1L1 use a homologous motif to recognize the H3/H4 tetramer.

Binding of APLF to the H3/H4 Tetramer Is Independent of Histone Tails

Next, we wanted to address whether the recognition of the histone tetramer by APLF is independent of the N-terminal histone tails, as previously observed for other histone

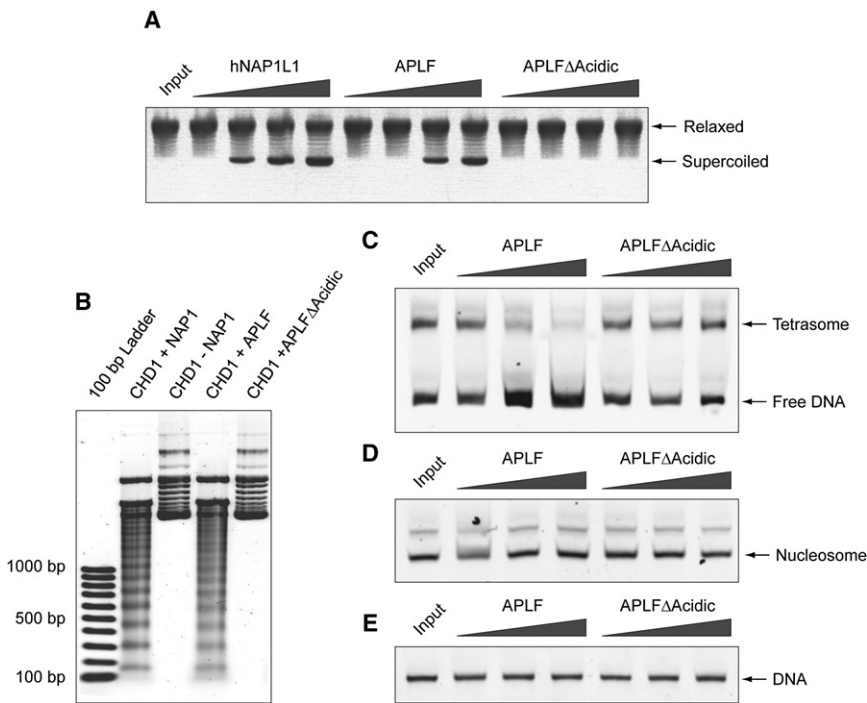


Figure 3. APLF Is a Histone Chaperone

(A) APLF facilitates chromatin assembly in a plasmid supercoiling assay in the presence of core histones and topoisomerase I.

(B) APLF assists CHD1 chromatin remodeler in chromatin formation as demonstrated by the appearance of a characteristic regularly spaced ladder of DNA fragments generated after partial nuclease digestion of the chromatin.

(C) APLF promotes chromatin disassembly by removing the histones from a tetrasome and leading to exposure of naked DNA.

(D and E) APLF has no effect on nucleosome or naked DNA substrates.

chaperones (Natsume et al., 2007; Zhou et al., 2008). To do this, we performed immunoprecipitation of the histone-associated complexes from HEK293T cells using FLAG-tagged histones H3 and H4, with or without N-terminal tails. The histones were coexpressed with myc-tagged WT APLF or mutant APLF lacking the C-terminal domain (APLF Δ Acidic), and their immunoprecipitates were analyzed for the presence of APLF using anti-myc antibody. The results in Figure 2E show that the histones lacking N-terminal tails pulled down the same amount of APLF as the full-length histones, suggesting that the tails are likely to be dispensable for this interaction. Thus, APLF and other histone chaperones employ a similar mode of histone recognition and primarily recognize histones through their globular domains.

APLF Is a Histone Chaperone

Next, we examined whether APLF exhibits any histone chaperone activities in vitro. First, we performed supercoiling assays on circular plasmid DNA using purified human histones in the presence of topoisomerase I. The result demonstrates that APLF facilitated chromatin assembly similarly to NAP1L1, leading to the generation of supercoiled DNA species (Figure 3A). In contrast, the APLF Δ Acidic mutant was unable to promote the formation of supercoiled DNA species in these assays, indicating inefficient chromatin assembly in the absence of the C-terminal domain. Second, we assessed the ability of APLF to aid the formation of well-ordered chromatin in an ATP-dependent chromatin assembly assay (Lusser et al., 2005). Briefly, core histones were loaded onto circular plasmid DNA via a histone chaperone and subsequently arranged into a regularly spaced chromatin array by the action of an ATP-dependent chromatin remodeling enzyme with nucleosome-spacing activity, in this case yeast CHD1. As seen in Figure 3, lane 2 CHD1 efficiently assembled

chromatin in the presence of *Drosophila melanogaster* NAP1, which is indicated by the characteristic regularly spaced ladder of DNA fragments generated after partial nuclease digestion of the chromatin (Figure 3B; lane 2). Conversely, this characteristic ladder was not observed in the absence of a histone chaperone (Figure 3B; lane 3). When we tested whether purified APLF can act as a histone chaperone in this reaction, we

observed that full-length APLF efficiently promoted the formation of regularly spaced chromatin in the presence of CHD1. Importantly, the APLF Δ Acidic mutant was unable to support the same reaction. Collectively, we have demonstrated that APLF exhibits typical histone chaperone activities in vitro and that these activities require the acidic C-terminal domain. Thus, APLF represents the mammalian core DNA break-repair factor with histone chaperone activity.

The fact that most of the known histone chaperones are involved in both chromatin assembly and disassembly prompted us to investigate the role of APLF in chromatin disassembly. To do so, we investigated the effect of APLF on dismantling nucleosomes and tetrasomes (H3/H4 tetramers assembled onto DNA). As shown in Figure 3C, we observed that incubation of full-length APLF with tetrasomes led to the loss of the tetrasome species and a concomitant increase in the amount of free DNA. In contrast, the same activity could not be observed with the APLF Δ Acidic mutant. Interestingly, equivalent amounts of APLF or APLF Δ Acidic had no effect on nucleosomes (Figure 3D) or naked DNA (Figure 3E). These results are concurrent with the in vivo preference of APLF for histone tetramers, and they suggest that the tetrasome, the most prominent intermediate formed during both chromatin assembly and disassembly, is the physiological substrate of APLF. In this regard, APLF may facilitate DNA repair by displacing histones or preventing the untimely reassembly of nucleosomes as recently demonstrated for NAP1 (Andrews et al., 2010).

The Acidic Domain of APLF Regulates Its Response to DNA Damage

APLF is a DNA damage response protein that is immediately recruited to the sites of DNA damage once the damage occurs

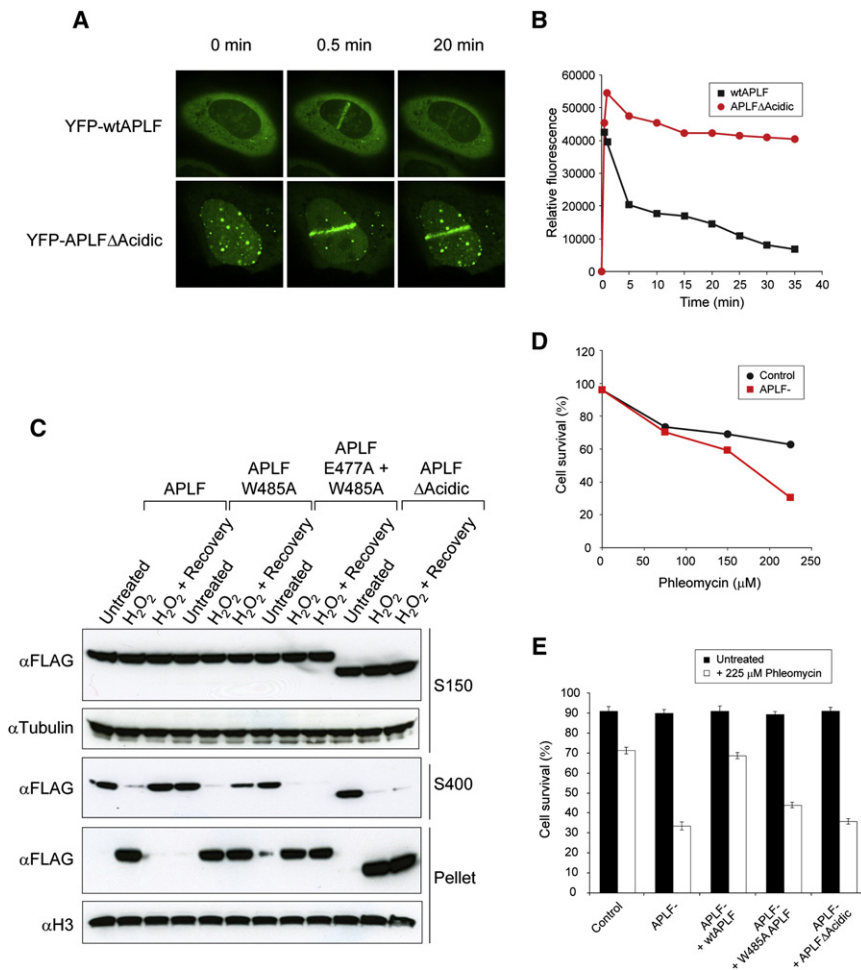


Figure 4. The Acidic Domain and NAP1L Motif of APLF Are Critical for Its DNA Repair Function

(A) Recruitment of wild-type YFP-APLF and YFP-APLF lacking the C-terminal acidic domain (APLF Δ Acidic) to the sites of laser-induced DNA damage. (B) Time course showing recruitment and disassociation of APLF and APLF Δ Acidic from sites of laser-induced DNA damage. The relative fluorescence values as shown in the graph were calculated by normalizing against background fluorescence intensity in the nucleus for the wild-type and mutant protein respectively. (C) APLF shifts from the soluble to the chromatin-bound fraction after H₂O₂ treatment. Retention of APLF variants with mutations in acidic domain in the chromatin following DNA damage is severely prolonged as compared to wt APLF. (D) FACS-based survival assays of U2OS cells stably transfected with control or APLF shRNAs and subjected to indicated doses of phleomycin. (E) APLF Δ Acidic and APLF mutated in the histone-binding NAP1L motif (W485A mutant) are unable to complement DNA repair deficiency of APLF⁻ cells as judged by FACS based live-dead cell analysis. The error bars represent s.d. (n = 3).

(Iles et al, 2007; Bekker-Jensen et al., 2007). To assess whether the C-terminal acidic domain of APLF affects its function in DNA damage response, we transiently expressed YFP-tagged APLF WT and APLF Δ Acidic in U2OS cells and compared their association/dissociation kinetics following laser-induced DNA damage using real-time confocal microscopy. The results in Figures 4A and 4B show that while the association of both proteins is similar, the retention of APLF Δ Acidic at the stripes of DNA damage was notably prolonged compared to the WT protein. Similarly, prolonged retention of APLF Δ Acidic in chromatin was observed by using biochemical fractionation following the treatment of cells with hydrogen peroxide (Figure 4C). Strikingly, the retention in chromatin was also prolonged for APLF proteins bearing point mutations in conserved residues of NAP1L motif (Figure 4C). Thus, the acidic domain of APLF and specifically NAP1L motif are important for the timely regulation of APLF in response to DNA damage.

The C-Terminal Acidic Domain of APLF Is Important for Efficient DNA Repair

APLF is involved in single- and double-strand break repair pathways. In repair of double-strand breaks APLF functions as a component of nonhomologous end-joining machinery (Rulten

et al., 2011). Appropriately, APLF deficiency was shown to lead to a moderate sensitivity to IR and camptothecin (Bekker-Jensen et al., 2007). In addition, we observed that knocking down the expression of APLF in U2OS cells induced sensitivity to the DNA damaging agent phleomycin (Figure 4D), judged by a FACS-based cell survival assay. At the concentrations tested, phleomycin produced notable amounts of double-strand breaks as judged by the appearance of H2AX and 53BP1 foci. Importantly, endogenous APLF colocalized well with both markers (Figure S2). We therefore explored the sensitivity of APLF-deficient cells to phleomycin and used the complementation strategy as a means to assess the importance of APLF's C terminus for efficient DNA repair. Our data showed that while the expression of shRNA-resistant WT-APLF fully complemented the sensitivity of APLF-deficient cells, the expression of APLF Δ Acidic or APLF W485A point mutant failed to restore the defect, highlighting the functional significance of the acidic tail and NAP1L motif in APLF-mediated DNA repair (Figures 4E and S3).

Interaction of APLF with Histones Is Modulated by DNA Damage

Next we investigated whether the interaction of APLF with histones is altered upon DNA damage. Strikingly, we observed that the interaction with H3 was notably increased after treatment with hydrogen peroxide, and that this was dependent on active poly(ADP-ribose) synthesis (Figure 5A). Furthermore, APLF exhibited selectivity toward certain H3 modifications after

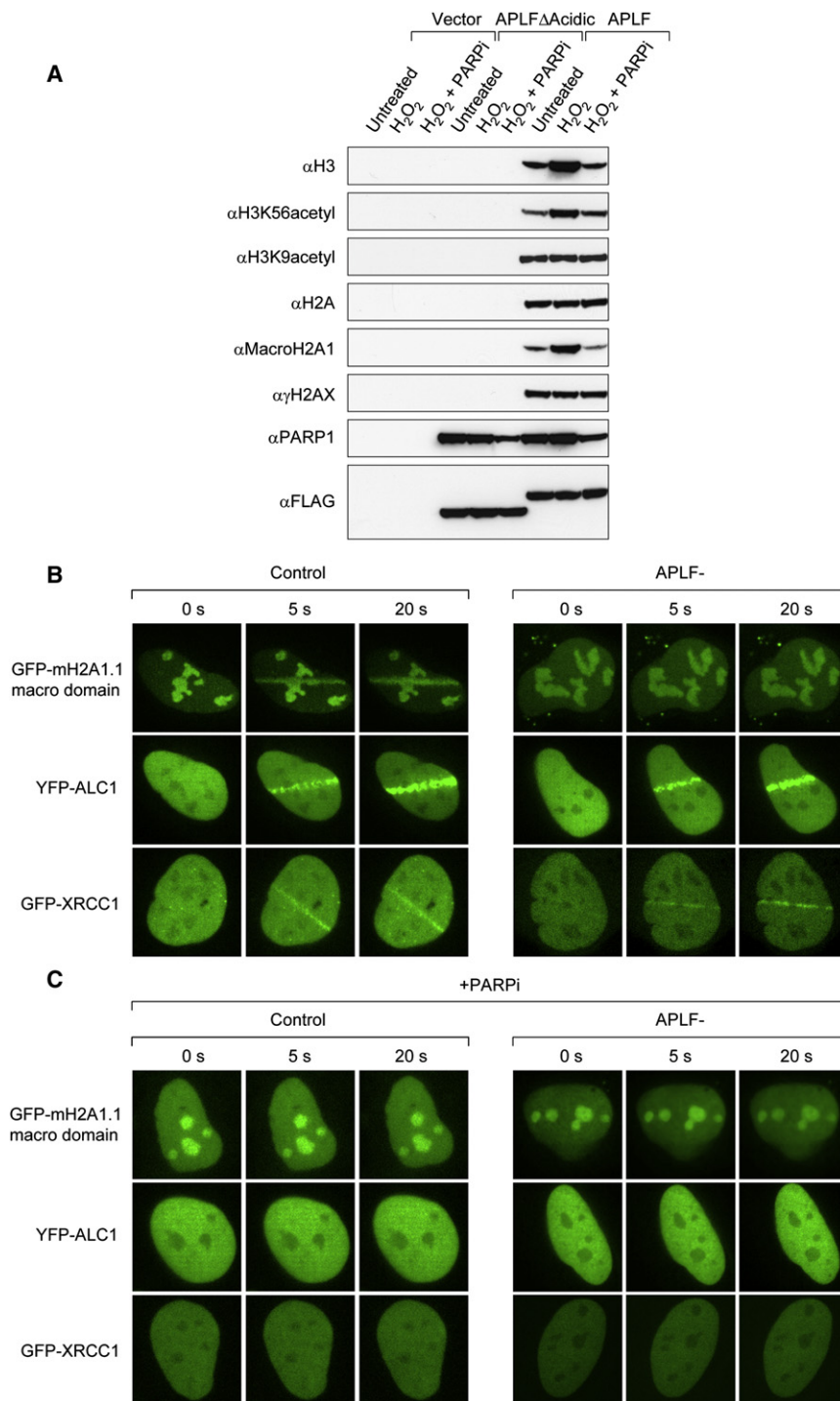


Figure 5. APLF Binds to MacroH2A1 and Shuttles Its Macrodomain to the Sites of DNA Damage

(A) Binding of APLF to histones is altered in response to DNA damage. This effect can be blocked by inhibiting active poly(ADP-ribose) synthesis. Complexes were purified by immunoprecipitation of transiently expressed FLAG-tagged APLF in HEK293T cells and analyzed by immunoblotting.

(B) Recruitment of fluorescently tagged macroH2A1 macro domain, ALC1, and XRCC1 to the sites of laser-induced DNA damage in APLF WT and APLF⁻ cells. Recruitment of macroH2A1 macrodomain to sites of DNA damage is dependent on presence of APLF.

(C) As for (B), but in the presence of PARP inhibitor.

and this was again dependent on active poly(ADP-ribose) synthesis. MacroH2A1 has been recently shown to sense PARP1 activation and rearrange chromatin following DNA damage (Timinszky et al., 2009), so it is possible that APLF plays a role in the recruitment/exchange of this histone variant at the sites of DNA damage.

Deposition of Macrodomain of MacroH2A1 to the Sites of DNA Damage Is Dependent on APLF

While visualizing the deposition and exchange of histones at the sites of DNA damage in vivo represents a major technical challenge, it was shown very recently that the isolated fluorescently tagged macrodomain of macroH2A1.1 variant promptly localizes to the sites of DNA damage (Timinszky et al., 2009), and we therefore hypothesized that its recruitment may be mediated by APLF. To investigate this possibility, we used WT and APLF-knockdown cells to analyze the recruitment of the macroH2A1.1 macrodomain to the stripes of laser-induced DNA damage as described (Timinszky et al., 2009). As shown in Figure 5B, in normal cells macrodomain of macroH2A1.1 promptly associated with DNA damage sites in a manner dependent on active

DNA damage, which was inferred by using modification-specific anti-H3 antibodies (Figure 5A; compare blots for H3K9 and H3K56 acetylation). Our results also show that unlike the association of APLF with H3, that with H2A was not affected by DNA damage. Instead, the interaction with the DNA damage responsive H2A variant macroH2A1 was greatly enhanced following the treatment with hydrogen peroxide,

PAR synthesis (Figure 5C). The kinetics of this association resembled that of other known PARP1-regulated DNA damage response factors such as ALC1 and XRCC1. Notably, in the case of the macrodomain of macroH2A1.1, this recruitment was ablated in APLF-deficient cells, whereas recruitment of ALC1 and XRCC1 was independent of the presence APLF. Thus, APLF is critical for the delivery of the macrodomain of

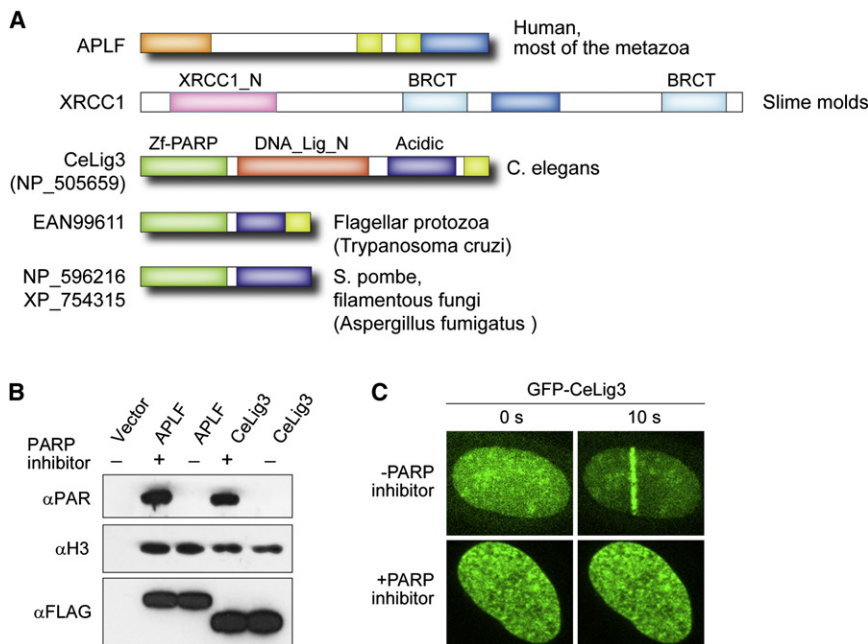


Figure 6. APLF Homologs and Analogs in Lower Eukaryotes

(A) Domain structures of the slime mold XRCC1 and the putative DNA repair factors containing zf-PARP DNA break sensor domain (named by accession numbers). Note that only acidic domain in XRCC1 of slime molds is homologous to APLF. (B) Western-blot showing that immunoprecipitated *C. elegans* zf-PARP protein CeLig3 binds to histones independently of poly(ADP-ribosylation). (C) Recruitment of GFP-tagged CeLig3 to the sites of laser-induced DNA damage is dependent on active poly(ADP-ribose) synthesis.

macroH2A1.1 to the sites of DNA damage. Taken altogether, our data suggest a possibility that APLF shuttles histones to the sites of DNA damage-induced poly(ADP-ribosylation), which is achieved through the cooperation of PBZ repeats acting as a DNA damage sensor and a histone-binding module. At the sites of DNA damage, APLF may further support the deposition or exchange of histone variants in facilitating DNA repair reactions.

Potential APLF Analogs in Lower Eukaryotes

APLF is present only in metazoans (excluding *C.elegans*); however, we reasoned that functional analogs of APLF might also be present in lower organisms. Analysis of the genomes of *C.elegans* and flagellate protozoa revealed putative DNA repair factors consisting of the DNA-break-sensor module called PARP zinc-finger (zf-PARP) (Petrucco and Percudani, 2008), an acidic domain (likely unrelated to APLF), and a PBZ zinc finger (Figure 6A). Moreover, similar proteins lacking the PBZ motif are also present in filamentous fungi and *Schizosaccharomyces pombe*. The Zf-PARP homolog from *C.elegans* (CeLig3) also possess the noncatalytic domain of DNA ligase III, and we previously demonstrated that this protein exhibits avid binding to PAR in vitro (Ahel et al., 2008). To assess whether CeLig3 binds histones and acts analogously to APLF as a DNA damage response protein, we transiently expressed tagged versions of CeLig3 in human HEK293T cells. We found that FLAG-tagged CeLig3 immunoprecipitated histones in a poly(ADP-ribose)-independent manner (Figure 6B; lanes 4 and 5). In addition, we observed prompt recruitment of GFP-tagged CeLig3 to the sites of laser-induced DNA damage. This recruitment was abolished by inhibition of active PAR synthesis (Figure 6C). Thus, functional analogs of APLF are present in lower eukaryotes, which further substantiates the importance of histone-binding domains in efficient DNA repair.

nance of chromatin integrity through its interaction with Cds1 checkpoint kinase and nap1 null mutant cells show temperature sensitivity as compared to wild-type cells (Grande et al., 2008). We used this phenotype as a simple assay to assess the physiological importance of NAP1L motif in mediating Nap1 protein function. WT Nap1 and a mutant containing mutations in the conserved residues of NAP1L motif (Figure 7A) were expressed in the wild-type and the mutant protein respectively both in WT and *nap1Δ* backgrounds. As shown in the western blot in Figure 7B, both the WT and mutant proteins expressed equally well; however, only the WT construct complemented the temperature sensitivity of the *nap1Δ* strain (Figure 7C). This result supports our findings on the APLF system and demonstrates the significance of the NAP1L histone-binding module in mediating specific protein functions.

Conclusion

In summary, we have established a function of APLF as a DNA-repair histone chaperone, and shown that histone chaperone-like domains are a conserved feature within eukaryotic DNA-repair pathways. In addition, we have provided insights into the molecular basis of histone recognition by histone chaperones in general. Collectively, our findings present a step toward a comprehensive understanding of the concerted actions of DNA repair factors in poly(ADP-ribose)-regulated repair of damaged chromatin.

EXPERIMENTAL PROCEDURES

Plasmids and Proteins

Human APLF, NAP1L1, XRCC1, mH2A1.1, H3.1, and H4 were amplified from a human HeLa cDNA library. *C. elegans* NP_505659 gene (CeLig3), APLF*PBZ mutant and ALC1 were cloned as described earlier (Ahel et al., 2008, 2009). All genes were cloned into the pDONR221 entry vector. Specific mutations were introduced using the QuickChange II site-directed mutagenesis kit

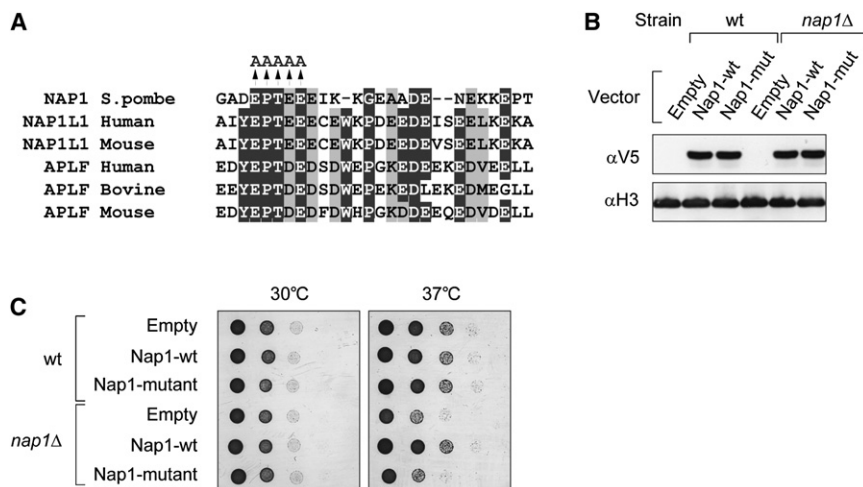


Figure 7. The APLF NAP1L Motif Is Important for the In Vivo Function of Nap1 in *S. pombe*

(A) Comparison of NAP1L motif in *S. pombe* Nap1 to the homologous motifs in vertebrate NAP1L1 and APLF proteins. Five conserved residues that were changed to alanines to inactivate *S. pombe* Nap1 are indicated by arrows.

(B) Immunoblot confirming expression of ectopically expressed Nap1 and Nap1 variant with the mutated NAP1L motif (Nap1 mutant) in *S. pombe* wt and *nap1Δ* cells.

(C) Nap1 variant with mutated NAP1L is unable to complement the temperature sensitivity phenotype as assessed by a spot growth test. Serial dilutions of equalized log-phase grown cultures of cells as indicated in the figure were plated on minimal media plates without uracil and colony formation was analyzed after 3 days at 30°C and 37°C.

(Stratagene). For the APLFΔAcidic mutant, the truncation was made to exclude amino acid residues 445–503. For the APLFΔFHA mutant, residues 1–350 were excluded, leaving the two PBZs and the acidic C terminus intact. For the tailless histones, residues 1–26 and 1–19 were excluded from H3 and H4, respectively. For transient transfections in human cells, the genes were recombined using the Gateway LR reaction (Invitrogen) into destination vectors for the expression of FLAG- or Myc-tagged proteins from the CMV promoter. For recombinant protein purification in *E. coli*, the APLF genes were recombined into pDEST15 vector for the expression of proteins with an N-terminal GST tag. Alternatively, APLF and NAP1L1 were expressed from pDEST17 vector for expression of N-terminally His-tagged proteins. All proteins were expressed in *E. coli* BL21-CodonPlus cells. The cultures were induced at 30°C with 0.2 mM IPTG for 2 hr. Recombinant proteins were purified over glutathione Sepharose beads (GE Healthcare) or Ni-NTA beads by standard protocols. The *S. pombe* Nap1 gene was amplified from genomic DNA isolated from the wild-type strain 972 and cloned into the expression vector pREP42 Pkc (ura marker) using the restriction sites NdeI and BamHI to express Nap1 protein with C terminus V5 tag.

Antibodies

Rabbit anti-APLF polyclonal antibody was raised against purified full-length recombinant APLF protein prepared from *E. coli*. Rabbit anti-PARP1, 53BP1, HP1α, γH2AX, H2A, H2B, H3, and H4 antibodies were obtained from Abcam. Rabbit anti-Ku80 was obtained from Serotec and mouse anti-FLAG antibody conjugated with peroxidase from Sigma-Aldrich. Mouse anti-myc-HRP antibody was purchased from Invitrogen. Rabbit anti-Acetyl-histone-H3(K9), acetyl-histone-H3(K56), macroH2A, and mouse γH2AX antibodies were obtained from Millipore. Goat anti-V5 antibody was bought from Genscript.

Cell Lines, Cell Culture, and Inhibitors

U2OS and HEK293T cell lines (ATCC) were maintained as adherent monolayers in DMEM media (GIBCO) containing 10% FBS and 1% Pen/Strep at 37°C in a humidified atmosphere of 5% carbon dioxide. Stable U2OS shAPLF and shControl cell lines were generated by transfection of the pLKO1 plasmid containing a hairpin targeting the translated region of APLF mRNA (sense target sequence [CAT CCT GGT GAT AGT GAT TAT]) or an empty vector. The cells were selected in media containing 2 μg/ml Puromycin (Sigma). shRNA-resistant variants of APLF were created using site directed mutagenesis utilizing the oligonucleotide 5'-attttagccatctcggagactccgactatg gagggtgtac-3' to introduce six silent mutations (underlined) in the coding region targeted by shRNA. These variants were then cloned into the pDEST12.2 vector (with a neomycin selection marker) for expression of the non-tagged APLF variants in the shAPLF background. The cells were selected in media containing 2 μg/ml puromycin (Sigma) and 500 μg/ml geneticin (Invitrogen).

PARP-1/2 inhibitor KU-0058948 was kindly provided by G.C. Smith (AstraZeneca).

Immunoblotting

Proteins were resolved on 4%–12% Bis-Tris gradient gels (Invitrogen) and transferred onto nitrocellulose membrane (GE Amersham). The membrane was blocked in PBS buffer supplemented with 5% non-fat dried milk. Proteins were detected with the appropriate primary antibodies and secondary antibodies coupled to horse-radish peroxidase (Pierce and DAKO) and subsequent development was with ECL western blotting detection reagent (GE Healthcare).

Immunoprecipitation

Human embryonic kidney 293T cells were transiently transfected using Polyfect transfection reagent (QIAGEN), according to the manufacturer's specifications. Following transfection (48 hr), cells were resuspended in lysis buffer (50 mM Tris-HCl pH 8.0, 150 mM NaCl, 1% Triton X-100, 1 mM dithiothreitol) supplemented with 50 U/μL benzamide nuclease (Sigma) and protease inhibitor cocktail (Roche). Whole-cell extracts were clarified by centrifugation and incubated with anti-FLAG M2 agarose (Sigma) for 20 min at 4°C. Following extensive washing with lysis buffer, the immunoprecipitates were boiled in SDS-PAGE loading buffer and analyzed by immunoblotting or mass spectrometry. Unless stated in the text specifically, all the IPs were washed with 150 mM NaCl. In the PARP inhibition experiments, HEK293T cells were pretreated with 0.5 μM KU-0058948 or PBS for 12 hr.

Biochemical Fractionation

APLF and mutants were transiently expressed in U2OS cells and were then either left untreated or treated with 0.5 mM H₂O₂ (sigma) for 15 min and immediately processed. To allow recovery from damage by H₂O₂, media containing H₂O₂ was aspirated off after 15 min, and fresh media were added. The cells were then allowed to recover for 1 hr, after which all the samples were fractionated into extracts by successive solubilisation in 150 and 400 mM salt as described previously (Ahel et al., 2009).

Mass Spectrometric Analyses and Protein Identification

Sypro Ruby stained protein bands were destained with 50% v/v acetonitrile and 50 mM ammonium bicarbonate, reduced with 10 mM DTT, and then alkylated with 55 mM iodoacetamide. Proteins were digested with 6 ng/μL trypsin overnight at 37°C. The digests were analyzed by nLCMSMS using a nanoACQUITY coupled to a SYNAPT HDMS (Waters, UK). Data-dependent analysis was carried out where automatic MS/MS was acquired on the eight most intense, multiply charged precursor ions in the m/z range 400–1500. LC/MS/MS data was searched against a concatenated, nonredundant protein database

(UniProt 13.6) using the Mascot search engine program V2.2 (Matrix Science, UK). Oxidation (Met), phosphorylation (STY), and carbamidomethylation (Cys) were included as variable modifications and a maximum of one missed tryptic cleavage was allowed. Precursor and fragment ion tolerances were set to 0.25 Da and 0.1 Da respectively.

GST Pull-Downs

Recombinant GST-tagged APLF and its mutant variants were purified on Glutathione Sepharose 4 Fast-Flow beads (GE Healthcare). GST-tagged proteins bound to the beads were incubated with recombinant *Xenopus laevis* histone tetramers in binding buffer (50 mM potassium phosphate, 600 mM NaCl, pH 7.2) for 1 hr. The beads were then extensively washed with binding buffer and subsequently with wash buffer (50 mM potassium phosphate, 1M NaCl), and the remaining proteins were then eluted with buffer containing 1.5 M NaCl.

Supercoiling Assay

Supercoiled pUC19 plasmid DNA isolated from log phase grown *E. coli* cultures was treated with topoisomerase I (Promega, Madison, WI, USA) to form relaxed DNA. HeLa core histones (200 ng) purchased from Millipore were preincubated in the presence or absence of 200, 400, 800, and 1200 ng of affinity purified NAP1L1, APLF, and the respective mutant proteins at 37°C for 15 min. After incubation, relaxed DNA (500 ng) was added to each reaction and further incubated at 37°C for 60 min, followed by 30 min of proteinase K digestion at 60°C. Plasmid DNA was then purified by ethanol precipitation and phenol:chloroform:isoamylalcohol protein extraction, separated on a 1% agarose gel for 3 hr at 50V in 1X TBE buffer and visualized by staining with ethidium bromide.

Chromatin Assembly Reaction

The chromatin assembly reaction was performed as described in the user manual of the Millipore Chromatin Assembly Kit. Instead of ACF1 as supplied by the manufacturer, recombinant yeast CHD1 (35 nM final concentration) was used for the assays. Recombinant *Drosophila* NAP1 and APLF (3 mg/ml) were used as histone chaperones to promote chromatin formation by CHD1.

Tetrasome Disassembly Assays

Nucleosomes and tetrasomes were assembled by performing salt-gradient dialysis on mixtures containing equimolar amounts of histone octamer or tetramer and 147 bp Cy3-labeled DNA containing the 601 nucleosome positioning sequence (Lowary and Widom, 1998). The tetrasome disassembly reactions were performed at 37°C by incubating tetrasomes, nucleosomes, or free DNA (1 μ M) in the absence or presence of increasing amounts of purified His-tagged APLF proteins (2.5, 5, and 10 μ g, respectively) in a reaction buffer of 50 mM Tris at pH 8, 150 mM NaCl, 0.5 mM DTT, and 1% glycerol for 1 hr in a final volume of 20 μ l. Reactions were stopped by the addition of 2 μ g of 1 kb DNA ladder (Promega) and sucrose to a final concentration of 5% (w/v), and the reaction mixtures were placed on ice prior to loading. The samples were run on a pre-run 0.5X TBE 5% native acrylamide gel at 150V at 4°C for 40 min. Bands were visualized on a Biorad Pharos FX plus imager with an excitation laser at 532 nm. The positions of nucleosomes, tetrasomes, and free DNA have been indicated in the figure.

ATPase Assay

The ATPase activity of ALC1 was measured in an assay as previously described (Ahel et al., 2009). 50 μ l ATPase reactions were carried out in 50 mM NaCl, 50 mM Tris HCl, pH 7.5 and 3 mM MgCl₂ with 0.09 μ M ALC1, 100 μ M ATP, and 20 μ M DNA and nucleosomes, NAD⁺ (50 μ M), PARP1 (3.2 nM), and PBP (3 μ M) in absence or presence of APLF and respective mutants (1.2 μ M) as shown in the figure.

Sensitivity to DNA Damage by FACS Analysis

Complemented stable cell lines (APLF WT and APLF Δ Acidic mutant) generated for the study were seeded into six well plates (100,000 cells/well), treated without or with 225 μ M final concentration of phleomycin (Melford), and grown for 3 days. After this, the cells were trypsinized and collected together with the media (containing dead cells) and were stained as per the specifications in the

Far Red (L10120) Live/Dead Fixable Cell Stain Kit (Invitrogen). The stained cells were analyzed by FACS (Calibur cytometer) using a laser with excitation at 635 nm with fluorescence emission monitored at 665 nm. The percent survival curves as shown in the figure were then generated using the FlowJo software.

Live-Cell Imaging by Laser Microirradiation

For generation of localized damage in cellular DNA by exposure to a UV-A laser beam, cells were plated on glass-bottom dishes and transfected using Polyfect (QIAGEN) 24 hr prior to laser damage. Cells were sensitized with 10 μ M 5-bromo-2'-deoxyuridine (BrdU, Sigma Aldrich) in phenol red-free medium (Invitrogen) for 24 hr at 37°C. Laser microirradiation was carried out on a spinning disk confocal microscope (Roper, France) based around a modified CSU22 scan head (Yokogawa, Japan) mounted upon an Olympus IX81 microscope equipped with an environmental chamber (Solent Scientific, UK) where CO₂/Air, temperature of the chamber and objective lens was maintained at 37°C. The sample was visualized with an Olympus UPLSAPO x100 1.45NA objective lens, excited with a 491 nm 50mW Solid State Laser (Cobolt AB, Sweden); detection occurred via a QuantEM 512B EMCCD camera (Roper AZ USA); equipment control and image capture was handled by Metamorph (Molecular Devices, CA, USA).

Laser irradiation was achieved via a 355 nm 10 mw CW Cobolt Zouk Laser entering the laser through the illumination port where the laser spot size at the point of focus was modulated to diameter of 300 nm at the sample and was translated across the sample via a series of computer controlled mirrors and lenses (Roper, France). Laser microirradiation across a nucleus was achieved in 1 s and image capture at a rate of 50 msec exposures every second so that detectable damage response was restricted to the laser path in a presensitization-dependent manner without noticeable cytotoxicity.

S.pombe Transformation and Spot Growth Test

Plasmid DNA comprising of pREP42pKC as vector backbone and harboring either wild-type or mutant nap1 were transformed into wild-type and nap1 Δ strains (bought from BIONEER Corporation, Korea) using lithium acetate protocol as described in Grande et al. (2008). Yeast transformants so obtained were grown in minimal media without uracil to log phase and then spotted on minimal media plates without uracil for assessing growth characteristics at 30°C and 37°C, respectively, after 3 days incubation. Total protein lysates for analyzing expression of the wild-type and mutant Nap1 protein(s) were prepared as described in Grande et al. (2008) and assessed using anti goat-V5 antibody.

SUPPLEMENTAL INFORMATION

Supplemental Information includes three figures and can be found with this article online at doi:10.1016/j.molcel.2010.12.008.

ACKNOWLEDGMENTS

We thank K. Labib, D. Neuhaus, S. Eustermann, and A. Bowman for helpful discussions, G. Smith (AstraZeneca) for the PARP inhibitor KU-0058948, I. Hagan, and E. Hartsuiker for help with *S. pombe* strains, and C. Tang for assistance with cell cultures. We are grateful to S. Bagley for technical support in the Paterson Advanced Imaging Facility and M. Blaylock for assistance in performing FACS analysis. We are also thankful to C. Wilkinson for providing the pREP42pKC vector. The work in I.A. laboratory is funded by Cancer Research UK. The laboratory of T.O.-H. is funded by a Wellcome Trust Senior Fellowship 064414. D.P.R. is supported by Australian National Health and Medical Research Council Biomedical (CJ Martin) Fellowship.

Received: May 12, 2010

Revised: July 16, 2010

Accepted: October 18, 2010

Published: January 6, 2011

REFERENCES

- Ahel, D., Horejsi, Z., Wiechens, N., Polo, S.E., Garcia-Wilson, E., Ahel, I., Flynn, H., Skehel, M., West, S.C., Jackson, S.P., et al. (2009). Poly(ADP-ribose)-dependent regulation of DNA repair by the chromatin remodeling enzyme ALC1. *Science* 325, 1240–1243.
- Ahel, I., Ahel, D., Matsusaka, T., Clark, A.J., Pines, J., Boulton, S.J., and West, S.C. (2008). Poly(ADP-ribose)-binding zinc finger motifs in DNA repair/checkpoint proteins. *Nature* 451, 81–85.
- Andrews, A.J., Chen, X., Zevin, A., Stargell, L.A., and Luger, K. (2010). The histone chaperone Nap1 promotes nucleosome assembly by eliminating non-nucleosomal histone DNA interactions. *Mol. Cell* 37, 834–842.
- Bekker-Jensen, S., Fugger, K., Danielsen, J.R., Gromova, I., Sehested, M., Celis, J., Bartek, J., Lukas, J., and Mailand, N. (2007). Human Xip1 (C2orf13) is a novel regulator of cellular responses to DNA strand breaks. *J. Biol. Chem.* 282, 19638–19643.
- D'Amours, D., Desnoyers, S., D'Silva, I., and Poirier, G.G. (1999). Poly(ADP-ribose)ylation reactions in the regulation of nuclear functions. *Biochem. J.* 342, 249–268.
- Eustermann, S., Brockmann, C., Mehrotra, P.V., Yang, J.C., Loakes, D., West, S.C., Ahel, I., and Neuhaus, D. (2010). Solution structures of the two PBZ domains from human APLF and their interaction with poly(ADP-ribose). *Nat. Struct. Mol. Biol.* 17, 241–243.
- Flaus, A., Martin, D.M., Barton, G.J., and Owen-Hughes, T. (2006). Identification of multiple distinct Snf2 subfamilies with conserved structural motifs. *Nucleic Acids Res.* 34, 2887–2905.
- Grande, M., Lambea, E., Fajardo, A., López-Avilés, S., Kellogg, D., and Aligue, R. (2008). Crosstalk between Nap1 protein and Cds1 checkpoint kinase to maintain chromatin integrity. *Biochim. Biophys. Acta* 1783, 1595–1604.
- Iles, N., Rulten, S., El-Khamisy, S.F., and Caldecott, K.W. (2007). APLF (C2orf13) is a novel human protein involved in the cellular response to chromosomal DNA strand breaks. *Mol. Cell Biol.* 27, 3793–3803.
- Kanno, S., Kuzuoka, H., Sasao, S., Hong, Z., Lan, L., Nakajima, S., and Yasui, A. (2007). A novel human AP endonuclease with conserved zinc-finger-like motifs involved in DNA strand break responses. *EMBO J.* 26, 2094–2103.
- Karras, G.I., Kustatscher, G., Buhecha, H.R., Allen, M.D., Pugieux, C., Sait, F., Bycroft, M., and Ladurner, A.G. (2005). The macro domain is an ADP-ribose binding module. *EMBO J.* 24, 1911–1920.
- Kim, M.Y., Zhang, T., and Kraus, W.L. (2005). Poly(ADP-ribose)ylation by PARP-1: 'PAR-laying' NAD⁺ into a nuclear signal. *Genes Dev.* 19, 1951–1967.
- Lowary, P.T., and Widom, J. (1998). New DNA sequence rules for high affinity binding to histone octamer and sequence-directed nucleosome positioning. *J. Mol. Biol.* 276, 19–42.
- Lusser, A., Urwin, D.L., and Kadonaga, J.T. (2005). Distinct activities of CHD1 and ACF in ATP-dependant chromatin assembly. *Nat. Struct. Mol. Biol.* 12, 160–166.
- Macrae, C.J., McCulloch, R.D., Ylanko, J., Durocher, D., and Koch, C.A. (2008). APLF (C2orf13) facilitates nonhomologous end-joining and undergoes ATM-dependent hyperphosphorylation following ionizing radiation. *DNA Repair (Amst.)* 7, 292–302.
- Natsume, R., Eitoku, M., Akai, Y., Sano, N., Horikoshi, M., and Senda, T. (2007). Structure and function of the histone chaperone CIA/ASF1 complexed with histones H3 and H4. *Nature* 446, 338–341.
- Park, Y.J., and Luger, K. (2006a). The structure of nucleosome assembly protein 1. *Proc. Natl. Acad. Sci. USA* 103, 1248–1253.
- Park, Y.J., and Luger, K. (2006b). Structure and function of nucleosome assembly proteins. *Biochem. Cell Biol.* 84, 549–558.
- Petrucco, S., and Percudani, R. (2008). Structural recognition of DNA by poly(ADP-ribose)polymerase-like zinc finger families. *FEBS J.* 275, 883–893.
- Pleschke, J.M., Kleczkowska, H.E., Strohm, M., and Althaus, F.R. (2000). Poly(ADP-ribose) binds to specific domains in DNA damage checkpoint proteins. *J. Biol. Chem.* 275, 40974–40980.
- Poirier, G.G., de Murcia, G., Jongstra-Bilen, J., Niedergang, C., and Mandel, P. (1982). Poly(ADP-ribose)ylation of polynucleosomes causes relaxation of chromatin structure. *Proc. Natl. Acad. Sci. USA* 79, 3423–3427.
- Rulten, S.L., Cortes-Ledesma, F., Guo, L., Iles, N.J., and Caldecott, K.W. (2008). APLF (C2orf13) is a novel component of poly(ADP-ribose) signaling in mammalian cells. *Mol. Cell Biol.* 28, 4620–4628.
- Rulten, S.L., Fisher, A.O., Robert, I., Zuma, M.C., Rouleau, M., Ju, L., Poirier, G., Reina-San-Martin, B., and Caldecott, K.W. (2011). PARP-3 and APLF Function Together to Accelerate Non-Homologous End Joining. *Mol. Cell* 41, this issue, 33–45.
- Timinszky, G., Till, S., Hassa, P.O., Hothorn, M., Kustatscher, G., Nijmeijer, B., Colombelli, J., Altmeyer, M., Stelzer, E.H., Scheffzek, K., et al. (2009). A macrodomain-containing histone rearranges chromatin upon sensing PARP1 activation. *Nat. Struct. Mol. Biol.* 16, 923–929.
- Zhou, Z., Feng, H., Hansen, D.F., Kato, H., Luk, E., Freedberg, D.I., Kay, L.E., Wu, C., and Bai, Y. (2008). NMR structure of chaperone Chz1 complexed with histones H2A.Z-H2B. *Nat. Struct. Mol. Biol.* 15, 868–869.